Clinical Radiology 74 (2019) 976.e1–976.e9

Contents lists available at ScienceDirect

Clinical Radiology

journal homepage: www.clinicalradiologyonline.net

Predicting gastro-oesophageal variceal bleeding in hepatitis B-related cirrhosis by CT radiomics signature

J.Q. Yang [a,b,1], R. Zeng [a,1], J.M. Cao [a,b,1], C.Q. Wu [a], T.W. Chen [a,*], R. Li [a,**], X.M. Zhang [a], J. Ou [a], H.J. Li [c], Q.W. Mu [b]

[a] *Sichuan Key Laboratory of Medical Imaging, Department of Radiology, Affiliated Hospital of North Sichuan Medical College, Nanchong 637000, Sichuan, China*
[b] *Department of Radiology, Nanchong Central Hospital/Second School of Clinical Medicine, North Sichuan Medical College, Nanchong 637000, Sichuan, China*
[c] *Department of Radiology, Beijing YouAn Hospital, Capital Medical University, Beijing 100069, China*

ARTICLE INFORMATION

Article history:
Received 13 April 2019
Accepted 30 August 2019

AIM: To develop liver a computed tomography (CT) radiomics model to predict gastro-oesophageal variceal bleeding (GVB) secondary to hepatitis B-related cirrhosis.

MATERIALS AND METHODS: Electronic medical records and image data of liver triple-phase contrast-enhanced CT examinations of 295 patients with hepatitis B-related cirrhosis were collected retrospectively from two hospitals. Two hundred and thirty-six and 59 patients were enrolled randomly into the training and validation cohorts, respectively; and 75 in the training cohort and 16 in the validation cohort endured GVB while the others did not during follow-up period. Radiomics features of the liver were extracted from the portal venous phase images, and clinical features came from medical records. The tree-based method and univariate feature selection were used to select useful features. The radiomics model, clinical model, and integration of radiomics and clinical models were built using the useful image features and/or clinical features. Predicting performance of three models was evaluated with the area under receiver-operating characteristic curve (AUC), accuracy, and F-1 score.

RESULTS: Twenty-one useful radiomics features and/or three clinical features were selected to build prediction models that correlated with GVB. AUC of integration of radiomics and clinical models was larger than of clinical or radiomics models for the training cohort (0.83±0.09 versus 0.64±0.08 or 0.82±0.10) and the validation cohort (0.64 versus 0.61 or 0.61). Integration of radiomics and clinical models obtained good performance in predicting GVB for both the training and validation cohorts (accuracy: 0.76±0.07 and 0.73, and F-1 score: 0.77±0.09 and 0.72, respectively).

* Guarantor and correspondent: T.W. Chen, Sichuan Key Laboratory of Medical Imaging, Department of Radiology, Affiliated Hospital of North Sichuan Medical College, 63# Wenhua Road, Nanchong 637000, Sichuan, China. Tel.: +86 817 2262236; fax: +86 817 2222856.
** Guarantor and correspondent: R. Li, Sichuan Key Laboratory of Medical Imaging, Department of Radiology, Affiliated Hospital of North Sichuan Medical College, 63# Wenhua Road, Nanchong 637000, Sichuan, China.
E-mail addresses: tianwuchen_nsmc@163.com, chentw@aliyun.com (T.W. Chen), ddtwg_nsmc@163.com (R. Li).
[1] These authors contribute equally to this work.

https://doi.org/10.1016/j.crad.2019.08.028

CONCLUSION: Integration of the radiomics and clinical models may be a non-invasive method to predict GVB.

Introduction

There are nearly 360 million hepatitis B virus carriers in the world.[1] About 20% of the carriers will develop chronic hepatitis, and of these patients, 50% with chronic hepatitis may develop cirrhosis. Cirrhosis of the liver will produce a series of complications, of which gastro-oesophageal variceal bleeding (GVB) is one of the most serious complications.[2] In patients with cirrhosis who survive the first bleed, the probability of rebleeding is 33–76% within the following year,[3] and it greatly increases mortality. Therefore, it is particularly important to predict the first GVB in patients with hepatitis B-related cirrhosis.

The first to fifth versions of the Baveno Consensus on portal hypertension have recommended regular endoscopy for portal hypertension patients because it is the only method that can directly observe varicose veins and measure their size[4]; however, endoscopy is an invasive examination, which will cause some pain to the patient, and may also cause bleeding of the oesophageal and gastric varices, and critically ill patients are generally intolerant. The sixth Baveno Consensus (Baveno VI) is the first to recommend the use of non-invasive tools, such as magnetic resonance imaging (MRI), computed tomography (CT), and Doppler ultrasound, to detect varicose veins at high risk of bleeding.[5] Doppler ultrasound is highly dependent on the examiner, so sensitivity is affected. MRI and CT have certain specificities, but MRI has some relative contraindications such as pacemakers and metal implants.

Radiomics is an emerging image-analysis technology that is increasingly receiving attention from radiologists and clinicians due to its innovative and quantitative advantages. This innovative approach first transforms medical images into high-dimensional quantitative features through post-processing techniques, and then performs image analysis. It uses a robust and repeatable method to comprehensively analyse these features and clinical data to get the final result, and avoids any differences between the inter- or intra-observers, is not related to the experience of the radiologist, making the results more objective, and it is a non-invasive examination that avoids unnecessary pain for the patients.[6–8] To the authors' knowledge, there is no literature to date regarding the determination of whether radiomics can better predict GVB secondary to cirrhosis. Therefore, the purpose of the present study was to explore and validate a radiomics model that predicts GVB secondary to hepatitis B-related cirrhosis.

Materials and methods

Patients

This retrospective study was approved by the institutional review board. Patient consent for the study was waived as it was retrospective and anonymised. This study was performed in accordance with the Declaration of Helsinki. Medical record review was performed in accordance with the guidelines of the institutional ethics review board.

The initial diagnosis of cirrhosis in patients with hepatitis B was based on physical findings, laboratory investigations, and imaging findings whenever available according to the American Association for the Study of Liver Diseases (AASLD) practice guidelines on chronic hepatitis B (2015).[9] Cases with hepatitis B were identified through laboratory investigations. During the period from January 2013 to February 2017, the records of 1,587 patients with a first-diagnosis of cirrhosis were collected from two hospitals, according to the following exclusion criteria: (1) complicated with liver cancer or other space-occupying lesions (n=626); (2) lost to follow-up (n=205); (3) previously received transjugular intrahepatic portosystemic shunt or other related surgery (n=67); (4) poor quality of CT images or incomplete clinical data (n=284); or (5) complicated with ulcerative gastrointestinal bleeding or primary haematological disease or other diseases, which might lead to gastrointestinal bleeding (n=110). In addition, the CT image quality was subjectively analysed on a five-point scale (1, worst; 2, suboptimal; 3, adequate; 4, very good; and 5, excellent) according to the image-quality scoring system.[10] If the score of the liver was three or more, the CT image could meet the requirements of the subsequent image segmentation for feature extraction. Patients were divided into GVB and non-GVB groups based on the GVB outcomes at telephone interview during the follow-up period. Patients without GVB were enrolled into the non-GVB group according to the following criterion: patients with first-diagnosed cirrhosis from January 2013 to February 2017 who were followed up by means of telephone and medical records in September 2018 to verify that patients had no GVB. Patients with GVB were enrolled into GVB group if patients with hepatitis B-related cirrhosis from January 2013 to February 2017 who were followed up by means of telephone interview and medical records in September 2018 to verify that patients had GVB. The questions asked at telephone interview were whether the patients had GVB or not, and whether the GVB was the first bleed or rebleeding. The mean follow-up period for the non-GVB group was 20.8±3.7

months (18.5–34.6 months), and the mean interval for the GVB group was approximately 22.5±4.3 months (range from 17.6 to 35.6 months). Consequently, the study involved 295 cases. Of all patients, 91 experienced GVB and 204 did not. All patients were divided randomly into two separate cohorts: the training cohort (n=236); and the validation cohort (n=59), among which 75 and 16 patients with GVB were assigned to the training cohort and the validation cohort, respectively. Relevant clinical data including gender, age, portal hypertension, and portal vein thrombosis were collected. Additionally, portal hypertension was identified according to the report: portal vein diameter of ≥13 mm; the formation of portosystemic collaterals, splenomegaly, and ascites are indirect indicators of portal hypertension.[11] The research sequence is illustrated in Fig 1.

Image acquisitions

All patients underwent abdominal contrast-enhanced CT with the two 128-section multidetector CT machines (SOMATOM Definition Flash, Siemens Healthcare systems, Germany) in two hospitals. During the abdominal CT, the patients were placed in supine position on the scanning bed and were instructed to take a deep aspiration and hold their breaths. After a routine unenhanced scan, the triple-phase contrast-enhanced CT was obtained using automatic scanning based on the trigger threshold of CT attenuation of 100 HU at the abdominal aorta, and started 20–30 seconds after the initiation of the injection of the contrast agent (iohexol; Omnipaque, GE Healthcare, Chicago, Illinois, USA) via a 20-G needle into an antecubital vein at a rate of 3 ml/s for a total of 80–100 ml calculated according to 2 ml/kg body weight with a pump injector, followed by a 20-ml saline flush. The arterial phase, portal vein phase, and delayed phase images were obtained 20–30, 50–60, and 90 seconds, respectively, after the contrast agent was injected. The CT imaging parameters for the unenhanced and contrast-enhanced scans were 140 kVp peak voltage, 240 mA tube current (automatic exposure control employed), section thickness of 5 mm, detector collimation of 128×0.125 mm, a pitch of 1.75, and a matrix of 512×512 mm. The coverage of CT scan was from the dome to the lower edge of the liver. The window width was set to 200 HU, and the window level was 50 HU. The image data were then transferred directly to the picture archiving and communication system. All images were exported in DICOM format for image feature extraction.

Image segmentation and feature extraction

The images used for the segmentation and feature extraction were all from the picture archiving and

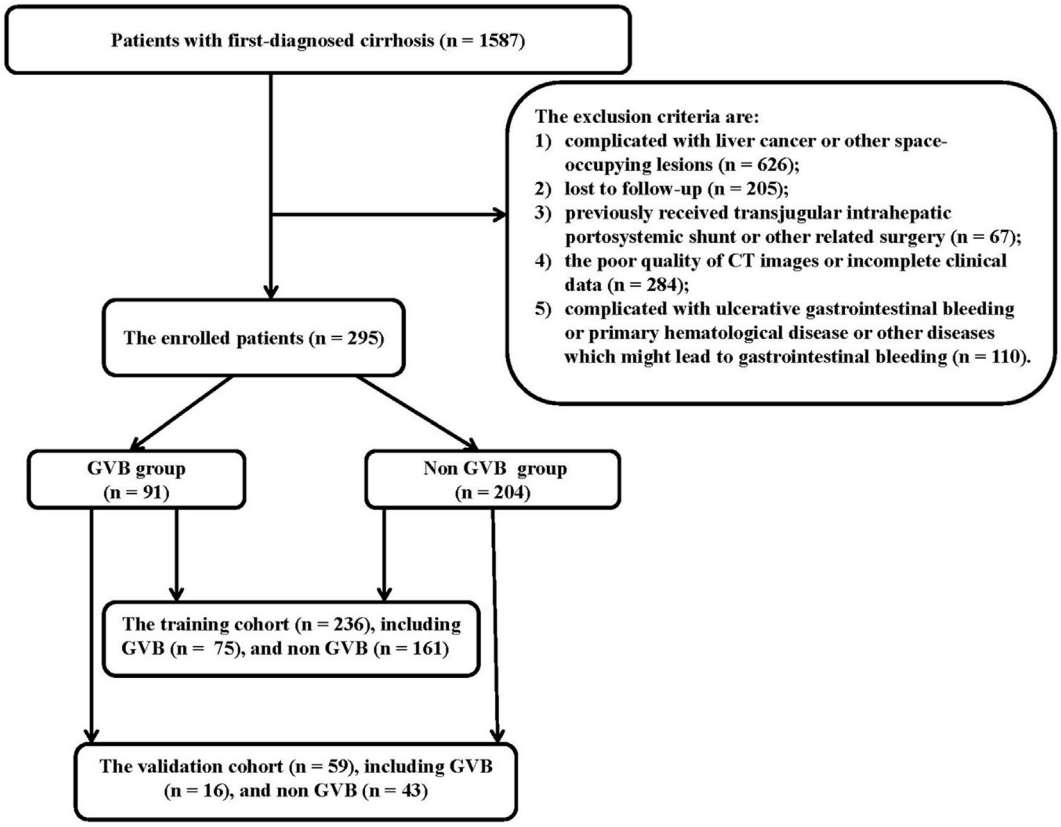

Figure 1 The CT data stream sequence in this study. Firstly, the entire liver contours are manually outlined layer by layer and relevant features are subsequently extracted. Then, in the training cohort, the effective features are selected. Based on the selected characteristics, the radiomics indicators are constructed and validated, and finally, the validation cohort is used to verify the predictive performance of the radiomics indicators. Ultimately, this study has shown that radiomics indicators can predict GVB secondary to hepatitis B-related cirrhosis.

communication system, and each patient's image data were set in the optimal window. Because the GVB could be best shown on the portal venous phase images when the triple-phase contrast-enhanced scans were performed, the image data from this phase were selected separately for the subsequent data analysis by two gastrointestinal radiologists (readers 1 and 2, with 6 and 8 years of experience, respectively, in gastrointestinal CT imaging) who were unaware of clinical information and laboratory tests.

For the segmentation of regions of interest (ROI) of the liver (Fig 2) and extraction of radiomics features, the entire liver was delineated by the above-mentioned two radiologists on the portal venous phase scans using the IBEX (β1.0, http://bit.ly/IBEX_MDAnderson) package (open source, source code version), which was developed in 64-bit MATLAB 2015b (Math Works).[12] The senior radiologist (T.W.C.) with 21 years of experience in gastrointestinal radiology checked all the returns on the previous two readers' investment on the portal venous phase images. Each ROI was as close as possible to the liver margin, but not beyond the liver margin, to avoid adjacent organs such as the gallbladder, intestine, stomach, spleen, kidney, and mesentery. When reader 1 and reader 2 disagreed, they reached a consensus after discussion, and the consensus was checked by the previous senior radiologist. In order to evaluate the reproducibility inside the observer, reader 1 repeated the ROI depiction twice in a week with the same procedure. The interobserver reproducibility was evaluated by the ROI segmentation of the previous readers 1 and 2. Based on the ROI, all feature extraction methods employed IBEX software using the in-house developed texture analysis algorithms. In this study, each patient produced 455 features from the portal venous phase images. These extracted features included the following key features: shape, intensity histogram, grey-level co-occurrence matrix (GLCM), and grey-level run length matrix (GLRLM) from the IBEX (Table 1).[12,13]

Because each ROI was separately delineated by two radiologists (readers 1 and 2), there could be a certain difference in the segmentation. The interobserver correlation coefficient (ICC_{inter}) was used to quantify the agreements of the 455 radiomics features extracted from the depicted ROIs by readers 1 and 2 separately. The intra-observer correlation coefficient (ICC_{intra}) was used to quantify the agreements of the 455 radiomics features extracted from the depicted ROIs by reader 1 twice. When both ICC_{inter} and ICC_{intra} were >0.75, radiomics feature extraction was considered to be reproducible.[14] All the image features were extracted, and were further processed to have zero mean and unit variance (z-score normalisation):

$$x_{norm} = \frac{x - \mu}{\sigma}$$

where x is the original feature value, μ is the mean value of this feature, and σ is its standard deviation.[15]

In the present study, the ratio of patients with and without GVB was 91:204, suggesting that the data were unbalanced. For the unbalanced data, it was difficult to obtain good results using traditional learning algorithms. It was therefore necessary to preprocess the data before machine learning using the training set so that there was no difference between patients with and without GVB, which could be achieved by oversampling.[16] Oversampling could improve the accuracy and recall of the model as shown by the tests on actual medical diagnostic data.[16,17] Oversampling was done by randomly selecting the patients with GVB for replication, thereby increasing the proportion of these participants.[16,18]

The following are the statistical analyses for radiomics feature selection. Each patient presented a large number of image features, but many of these features might be just noise or highly correlated with each other, so features needed to be reduced to select subsets of useful and unique features to improve prediction accuracy and minimise computational cost.[19] Tree-based estimators were chosen to select the most useful image features for predicting GVB, and then all selected features were tested using an independent sample t-test or chi-square Kruskal–Wallis H test. The importance of each feature was evaluated by p-value, leaving only the features with a p-value <0.05. Four clinical factors possibly associated with GVB secondary to cirrhosis, including gender, age, portal hypertension, and portal vein thrombosis, were also collected. Statistical analysis was also performed using the t-test or chi-square Kruskal–Wallis H test to determine whether these clinical features were statistically significant for prediction of GVB.

The previous selected radiomics and clinical features were used to construct three predictive models through random forest, including a radiomics model, a clinical model, and an integration of the radiomics and clinical features. The training process was optimised by the 10-fold cross-validation and grid search method to obtain an optimal training result, and then the performance of the model was tested through the test set. Training results and test results were evaluated using three differentiating indicators including area under the receiver operating characteristic curve (AUC), accuracy, and F-1 score.

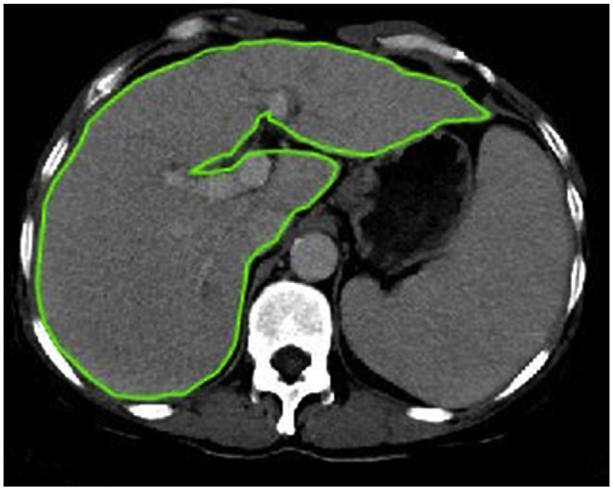

Figure 2 The liver contours are manually outlined on the contrast-enhanced portal venous phase CT data.

Table 1
Feature extraction.

	Radiomics features
Shape	The shape presents descriptors of the three-dimensional size and shape of the liver, including the following: tightness 1, firmness 2, convex, convex volume (CHV), convex volume 3D (CHV3D), mass, maximum 3D diameter (M3DD), average width (MB), number of voxels, direction, roundness, spherical inhomogeneity (SD), sphericity, surface area (SA), surface area density, (SAD) and volume
Intensity histogram	The intensity histogram mainly includes the following contents: interquartile range, kurtosis, mean absolute deviation (MAD1), median absolute deviation (MAD2), percentile, percentile area, points Number of digits, range, and skewness
GLCM	GLCM describes general information of intensity levels of CT images in different directions and offsets and arrangement pattern of different voxels. In this study, each GLCM feature was measured by four directions (θ=0°, 45°, 90°, 135°) and three offsets (d =1, 4, 7), including the following: autocorrelation, dissimilarity, energy, entropy, homogeneity 1, homogeneity 2, max probability (MA), sum average (SA), sum entropy and sum variance
GLRLM	GLRLM quantifies grey level runs in CT images. In this study, each GLRLM feature was measured by two directions (θ=0°, 90°) and one offset (λ = 1), including the following: grey-level non-uniformity, high grey-level run emphasis, long run emphasis, long run high grey-level emphasis, long run low grey-level emphasis, low grey-level run emphasis, run-length non-uniformity, run percentage, short run emphasis, short run high grey-level emphasis, and short run low grey-level emphasis

GLCM, grey-level co-occurrence matrix; and GLRLM, grey-level run length matrix.

Statistics

All statistical analyses were conducted using R (Version 3.4.1, https://www.r-project.org/). The reported statistical significance levels were bilateral, with a *p*-value of <0.05 indicating statistical difference.

The correlation coefficient was used to quantify the intra-observer and interobserver agreements for each of the extracted 455 radiomics features. Clinical characteristics were measured based on the type of variable. The Shapiro–Wilk test was used to assess the normality of the feature distribution, and the uniformity of the variance was tested by the Bartlett test. Continuous variables were expressed as mean or median, and compared by independent *t*-test. The categorical variables were measured in proportion, and compared using a chi-square test. The tree-based estimators were performed using R software version 3.4.4 (https://www.r-poject.org), and other analyses were done using python 3.6 (http://www.python.org).

Results

Baseline clinical independent predictors for GVB

A total of 295 patients were recruited, and the specific clinical features are shown in Table 2. With regards to the relevant clinical information, there were statistical differences in gender, portal hypertension, and portal vein thrombosis between cirrhosis patients with and without GVB, indicating that these three clinical indexes could be used to establish a model to predict GVB (Table 3). The *p*-value was >0.05 in age, suggesting no statistical difference in this index between patients with and without GVB.

Intra- and interobserver variability in assessment of image features extraction

For the intra- and interobserver agreements of features extraction, ICC_{intra} and ICC_{inter} were >0.75 for the extraction of 445 features while either ICC_{intra} or ICC_{inter} was less than 0.75 for that of the remained 10 features, indicating that the previous 445 features extracted by reader 1 could be reproducible. The 445 features from reader 1 with both ICC_{intra} and ICC_{inter} >0.75 were used to build a multivariate predictive model.

Feature selection and radiomics signature building

From the 445 image features extracted by reader 1 with both ICC_{intra} and ICC_{inter} >0.75, 50 useful features were selected by the tree-based method (9.1:1 ratio) as shown in Fig 3. Based on the *t*-test or chi-square

Table 2
Clinical characteristics of enrolled patients.

	The training cohort		The validation cohort	
	With GVB (*n*=75)	Without GVB (*n*=161)	With GVB (*n*=16)	Without GVB (*n*=43)
Median age (year)	58.08 (40–85)	58.24 (15–99)	56.31 (33–81)	61.67 (23–81)
Gender (%)				
Male	45 (60)	102 (63.4)	13 (81.3)	27 (62.8)
Female	30 (40)	59 (36.6)	3 (18.7)	16 (37.2)
Portal hypertension (%)				
Yes	42 (56)	93 (57.8)	9 (56.3)	21 (48.8)
No	33 (44)	68 (42.2)	7 (43.7)	22 (51.2)
Portal vein thrombosis (%)				
Yes	16 (21.3)	9 (5.6)	5 (31.3)	4 (9.3)
No	59 (78.8)	152 (94.4)	11 (68.7)	39 (90.7)

GVB, gastro-oesophageal variceal bleeding.

Table 3
Selected features with description.

Feature name	*p*-Value
Image feature	
Max 3D diameter	0.001
X0.025 quantile	0.007
Roundness	0.046
X90 low grey-level run emphasis	0.005
Number of voxel	0.015
X.333 short run low grey-level emphasis	0.017
Convex hull volume	0.008
Surface area	0.028
Volume	0.019
X90SRGLG	0.016
X5 percentile	0.024
X45.7 contrast	0.026
X0 low grey-level run emphasis	0.002
Convex hull volume 3D	0.017
X90 high grey-level run emphasis	0.018
X0 short run low grey-level emphasis	0.031
X45.4 inverse diff moment norm	0.032
X45.4 contrast	0.027
X45.7 inverse diff moment norm	0.031
Texture strength	0.021
X135.4 cluster prominence	0.020
Clinical feature	
Sexy	0.009
Portal vein thrombosis	<0.001
Portal hypertension	0.015

Kruskal–Wallis H test, a total of 21 important image features were ultimately selected for predicting GVB (Table 3).

Model construction and prediction performance

The 21 selected image features and three selected clinical features were applied to develop three diagnostic models for prediction of GVB by using the training cohort. The three predictive models included a radiomics model, a clinical model, and a model created by integrating the radiomics and clinical features. The most suitable model was selected based on the receiver operating characteristic (ROC) curves illustrated in Fig 4, together with the AUC, accuracy, and F-1 score as shown in Table 4. Through the integration of radiomics and clinical features, the model was superior to either of the other two models for prediction of GVB secondary to hepatitis B-related cirrhosis.

Discussion

The increasing popularity of precision medicine has led to the emergence and development of radiomics. Radiomics uses state-of-the-art machine learning techniques to quickly extract large quantities of quantitative features from CT, MRI or positron-emission tomography, convert these quantitative features into usable data, and then analyse and develop a medical model using sophisticated bioinformatics tools.[20–22] This model can predict the occurrence of disease and improve the accuracy of diagnosis. This study was carried out to develop and validate a radiomics model for prediction of GVB secondary to hepatitis B-related cirrhosis. Based on abdominal contrast-enhanced CT images and/or

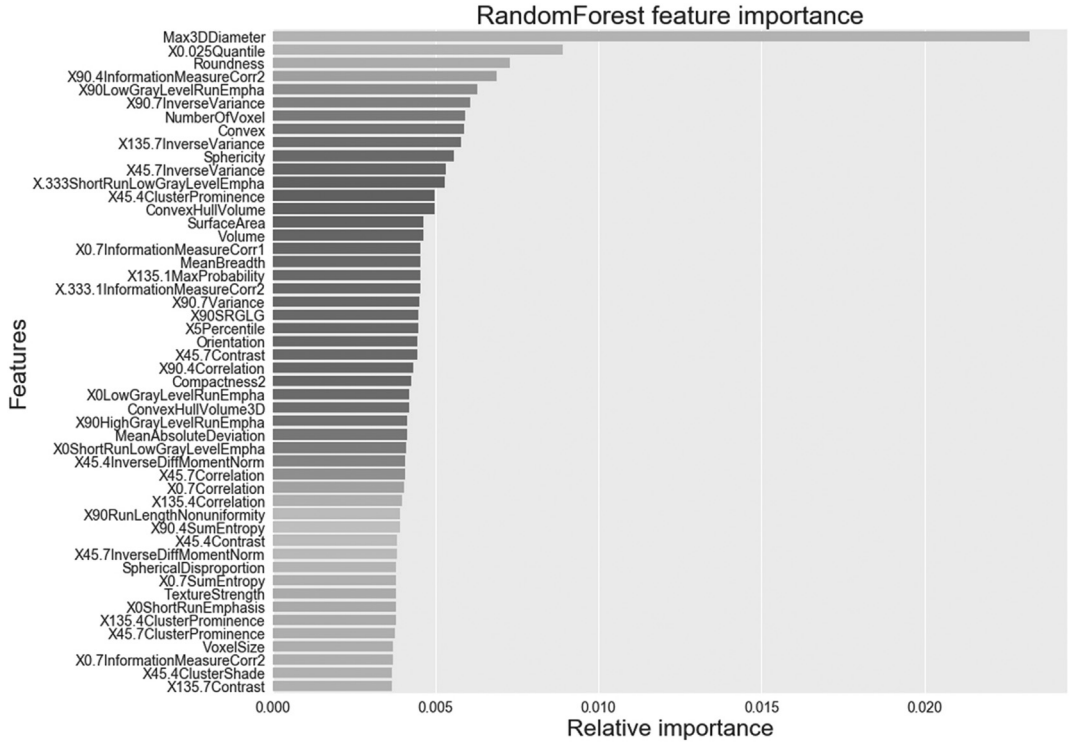

Figure 3 The tree-based method used in this study for the radiomics feature extraction. The tree-based method has the greedy nature of step-by-step node splitting, and also has "grouping properties", which enables the tree to skilfully handle the correlation and interaction between variables. In this study, a tree-based method is used to screen out 50 related features from the 445 radiomics candidate features. These 50 radiomics features are shown to be associated with the prediction of GVB secondary to cirrhosis.

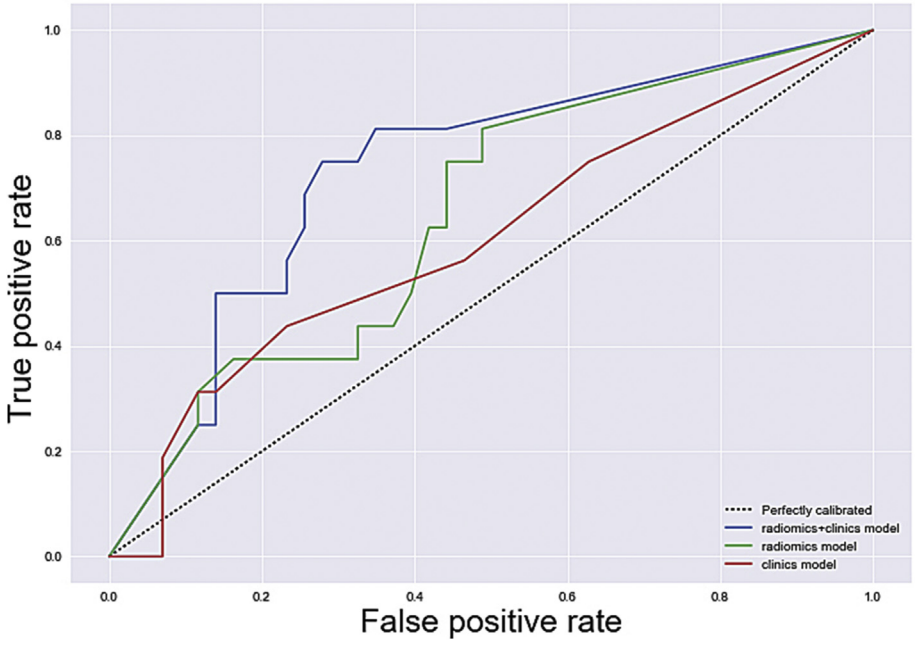

Figure 4 The ROC curves of the integration of both radiomics and clinical model, the clinical model, and the radiomics model have been obtained to predict GVB secondary to hepatitis B-related cirrhosis in the validation cohort.

Table 4
Performance of the models in training and validation cohorts.

Prediction model	AUC	Accuracy	F-1 score
The training cohort			
Integration of both radiomics and clinical model	0.83±0.09	0.76±0.07	0.77±0.09
Radiomics model	0.82±0.10	0.74±0.10	0.75±0.10
Clinical model	0.64±0.08	0.61±0.09	0.67±0.09
The validation cohort			
Integration of both radiomics and clinical model	0.64	0.73	0.72
Radiomics model	0.61	0.66	0.66
Clinical model	0.61	0.54	0.57

AUC, area under receiver operating characteristic curve.

clinical features, three predictive models were developed and validated, including a radiomics model, a clinical model, and a model created by integrating the radiomics and clinical features for prediction of GVB secondary to hepatitis B-related cirrhosis. The present study showed that the model of integrating both radiomics and clinical features could be better than the clinical or radiomics models for prediction of GVB, indicating that this integrated model is promising for clinical use so as to alert high-risk patients with GVB secondary to cirrhosis.

As shown in the present study, independent clinical risk factors for GVB secondary to cirrhosis observed in both training and validation cohorts included gender, portal hypertension, and portal vein thrombosis. Gender can be an independent predictor, which can be explained by the difference in the incidence of cirrhosis between men and women. The incidence of cirrhosis in men may be significantly higher than in women (men versus women: 187 versus 108). The presence and severity of oesophageal varices depend on the severity of portal hypertension secondary to cirrhosis,[23] indicating that portal hypertension could be a clinical risk factor for GVB. In addition, portal thrombosis can be an independent predictor, which may be related to the cause of portal hypertension; however, when a clinical model containing only clinical features is established to predict GVB, its performance cannot be satisfactory in the training and validation cohorts.

A radiomics model using the selected 21 image features was developed for predicting GVB, showing a slightly better performance compared with the above-mentioned clinical model. In order to improve the performance for prediction of GVB, integration of both radiomics and clinical models was undertaken. The findings show that the performance of the integrated model is better than that of either the radiomics model or the clinical model for prediction of GVB because of higher AUC, accuracy, and F-1 score observed for both the training and validation cohorts. This finding can be explained in that the radiomics features complement the relevant clinical features to improve the predictive performance.[20,21,24] Since the sixth Baveno Consensus (Baveno VI) on portal hypertension recommends the use of non-

invasive tools such as CT to detect varicose veins at high risk of bleeding,[5] the present study suggests the integration of both CT radiomics and clinical models as a new non-invasive tool for screening cirrhotic patients with a higher risk of GVB.

The following aspects ensure the robustness of the radiomics and clinical models. When contrasted with the traditional practice of treating medical images only as visually interpreted images, the radiomics model can improve the accuracy of prediction. In addition, the radiomics model is a quantitative analytic model that is independent of subjective analysis.[22] In the present study, the correlation coefficient of the intra- and interobserver agreements of the 445 image feature extraction is >0.75, suggesting a high degree of stability can be found in the useful radiomics features for prediction of GVB.

On the other hand, the feature extraction process produces a large number of features; however, a number of features is useless, and selecting the useful features and eliminating the redundant features can improve the performance of the predictive model.[22] In the present study, the tree-based method and *t*-test or chi-square Kruskal–Wallis H test have been used to select the texture features, and 21 of the 445 candidate features have been selected to be most relevant to GVB secondary to cirrhosis, which ensures the importance and independence of each feature in the ultimate model. The three clinical features are also screened with *t*-test or chi-square Kruskal–Wallis H test to predict GVB. Random forest was used in the present study to build the models for predicting GVB, which is based on the principle that random forest is a tree-based ensemble machine learning tool, and the tree has a "grouping property" that enables random forest to quickly handle correlations between variables, using variable importance for feature selection and sorting.[25]

In addition, the GVB prediction model has uniqueness. Unlike the prediction model that only contains radiomics features, this multivariate model was developed by integration of radiomics and clinical features, and improved the performance of GVB prediction for precise intervention of cirrhotic patients with a higher risk of GVB. Compared with the referenced study regarding the prediction of oesophageal varices in cirrhotic patients with apparent diffusion coefficient of the spleen,[26] the present results for GVB in cirrhotic patients have been derived from the training cohort and have been validated in the testing cohort while the results in this published study have not been validated, indicating that the present results could be more reliable.

This study has several limitations. Firstly, the sample size was relatively small, because the aim was to ensure data consistency and CT data from the same scanner using the same scanning parameters were selected. This predictive model will be validated using CT data from different scanners in other hospitals as the next step, and multicentre validation will be undertaken to confirm the present findings. Secondly, new radiomics features discovered by deep learning were not considered. The radiology combination function with deep learning discovery function can further improve the prediction accuracy automatically.[7,13] Thirdly, there is a high drop-off rate of patients in this study. Cirrhotic patients were excluded, as listed in the exclusion criteria, in order to keep the accuracy of the extracted CT radiomics features of hepatitis B-related cirrhosis. Although this high drop-off rate might not have introduced bias, the present findings will be confirmed in a future prospective study. Fourthly, genotyping of cirrhosis was not considered. As demonstrated in the published studies regarding cirrhosis in patients with chronic hepatitis C, multiple genes interacting with environmental factors could affect the progression of liver fibrosis.[27,28] Radiogenomics is concerned with the relationship between imaging radiomics and genomics. Establishing whether a radiogenomics model is superior to a radiomics model for prediction of GVB has yet to be undertaken.

In summary, a multivariate model was developed based on the CT features and related clinical features that showed good accuracy in predicting GVB secondary to hepatitis B-related cirrhosis. It is hoped that the present model can help predict the possibility of GVB secondary to hepatitis B-related cirrhosis for timely treatment decision-making, and can help to develop the predictive model for GVB in patients with cirrhosis from other causes.

Conflict of interest

The authors declare no conflict of interest.

Acknowledgements

The authors thank Dr Xin Li from GE Healthcare for teaching us how to extract imaging features. This study was supported by the Nanchong-University Cooperative Research Project (grant no. NSMC20170206) funded by Science and Technology Bureau of Nanchong City solely for the conduct of the research.

References

1. Lv Y, Yee Lau W, Wu H, *et al*. Causes of peripheral cytopenia in hepatitic cirrhosis and portal hypertensive splenomegaly. *Exp Biol Med (Maywood)* 2017;**242**:744–9.
2. Ibrahim M, Mostafa I, Devuere J. New developments in managing variceal bleeding. *Gastroenterology* 2018;**154**:1964–9.
3. Baiges A, Hernández-Gea V, Bosch J. Pharmacologic prevention of variceal bleeding and rebleeding. *Hepatol Int* 2018;**12**:68–80.
4. Moctezuma Velazquez C, Abraldes JG. Non-invasive diagnosis of esophageal varices after Baveno VI. *Turk J Gastroenterol* 2017;**28**:159–65.
5. de Franchis R. Non-invasive (and minimally invasive) diagnosis of oesophageal varices. *J Hepatol* 2008;**49**:520–7.
6. Hou Z, Li S, Ren W, *et al*. Radiomic analysis in T2W and SPAIR T2W MRI: predict treatment response to chemoradiotherapy in esophageal squamous cell carcinoma. *J Thorac Dis* 2018;**10**:2256–67.
7. Yang X, Pan X, Liu H, *et al*. A new approach to predict lymph node metastasis in solid lung adenocarcinoma: a radiomics nomogram. *J Thorac Dis* 2018;**10**:S807–19.
8. Peikert T, Duan F, Rajagopalan S, *et al*. Novel high-resolution computed tomography-based radiomic classifier for screen-identified pulmonary nodules in the National Lung Screening Trial. *PLoS One* 2018;**13**:e0196910.
9. Terrault NA, Bzowej NH, Chang KM, *et al*. American Association for the Study of Liver Diseases. AASLD guide-lines for treatment of chronic hepatitis B. *Hepatology* 2016;**63**:261–83.

10. Chen TW, Yang ZG, Dong ZH, *et al*. Whole tumour first-pass perfusion using a low-dose method with 64-section multidetector row computed tomography in oesophageal squamous cell carcinoma. *Eur J Radiol* 2011;**80**:284–91.
11. Shastri M, Kulkarni S, Patell R, *et al*. Portal vein Doppler: a tool for non-invasive prediction of esophageal varices in cirrhosis. *J Clin Diagn Res* 2014;**8**:MC12–5.
12. Zhang L, Fried DV, Fave XJ, *et al*. IBEX: an open infrastructure software platform to facilitate collaborative work in radiomics. *Med Phys* 2015;**42**:1341–53.
13. Peng J, Zhang J, Zhang Q, *et al*. A radiomics nomogram for preoperative prediction of microvascular invasion risk in hepatitis B virus-related hepatocellular carcinoma. *Diagn Interv Radiol* 2018;**24**:121–7.
14. Noh T, Griffith B, Snyder J, *et al*. Intraclass correlations of measured magnetic resonance imaging volumes of laser interstitial thermal therapy-treated high-grade gliomas. *Lasers Surg Med* 2019 Jun 28, https://doi.org/10.1002/lsm.23111 [Epub ahead of print].
15. Abdi H. Encyclopedia of research design. In: Salkind N, editor. *Normalizing data*. Thousand Oaks, CA: Sage; 2010. p. 1–4.
16. Han W, Huang Z, Li S, *et al*. Distribution-sensitive unbalanced data oversampling method for medical diagnosis. *J Med Syst* 2019;**43**:39.
17. Wang X, Yu B, Ma A, *et al*. Protein–protein interaction sites prediction by ensemble random forests with synthetic minority oversampling technique. *Bioinformatics* 2019 Jul 15;**35**(14):2395–402.
18. Vaughan R. Oversampling in health surveys: why, when, and how? *Am J Public Health* 2017;**107**:1214–5.
19. Zhang Y, Oikonomou A, Wong A, *et al*. Radiomics-based prognosis analysis for non-small cell lung cancer. *Sci Rep* 2017;**7**:46349.
20. Gillies RJ, Kinahan PE, Hricak H. Radiomics: images are more than pictures, they are data. *Radiology* 2016;**278**:563–77.
21. Permuth JB, Choi J, Balarunathan Y, *et al*. Combining radiomic features with a miRNA classifier may improve prediction of malignant pathology for pancreatic intraductal papillary mucinous neoplasms. *Oncotarget* 2016;**7**:85785–97.
22. Acharya UR, Hagiwara Y, Sudarshan VK, *et al*. Towards precision medicine: from quantitative imaging to radiomics. *J Zhejiang Univ Sci B* 2018;**19**:6–24.
23. Zhou H, Zhang J, Zhang X, *et al*. Liver volume measured on magnetic resonance imaging in cirrhosis patients with hepatitis B: association with severity of esophageal varices. *Int J Clin Exp Med* 2017;**10**:9495–501.
24. Zhang B, Tian J, Dong D, *et al*. Radiomics features of multiparametric MRI as novel prognostic factors in advanced nasopharyngeal carcinoma. *Clin Cancer Res* 2017;**23**:4259–69.
25. Chen X, Ishwaran H. Fandom forests for genomic data analysis. *Genomics* 2012;**99**:323–9.
26. Razek AA, Massoud SM, Azziz MR, *et al*. Prediction of esophageal varices in cirrhotic patients with apparent diffusion coefficient of the spleen. *Abdom Imaging* 2015;**40**:1465–9.
27. Besheer T, Arafa M, El-Maksoud MA, *et al*. Diagnosis of cirrhosis in patients with chronic hepatitis C genotype 4: role of ABCB11 genotype polymorphism and plasma bile acid levels. *Turk J Gastroenterol* 2018; **29**:299–307.
28. Besheer T, Elbendary M, Elalfy H, *et al*. Prediction of fibrosis progression rate in patients with chronic hepatitis C genotype 4: role of cirrhosis risk score and host factors. *J Interferon Cytokine Res* 2017;**37**:97–102.